Antenna for Ultrawideband Channel Sounding

Zhekov, Stanislav Stefanov; Tatomirescu, Alexandru; Pedersen, Gert F.

Published in:
I E E E Antennas and Wireless Propagation Letters

DOI (link to publication from Publisher):
10.1109/LAWP.2016.2600245

Publication date:
2016

Document Version
Accepted author manuscript, peer reviewed version

Antenna for Ultrawideband Channel Sounding

Stanislav Stefanov Zhekov, Alexandru Tatomirescu, and Gert Frølund Pedersen

***Abstract*—A novel compact antenna for ultrawideband channel sounding is presented. The antenna is composed of a symmetrical biconical antenna modified by adding a cylinder and a ring to each cone. A feeding coaxial cable is employed during the simulations in order to evaluate and reduce its impact on the antenna performance. The optimized antenna demonstrates S_{11} below -10 dB and a stable omnidirectional radiation pattern robust against the cable effect over the frequency band 1.5-41 GHz despite its compactness (the maximum electrical dimension is of $0.29\lambda_{max}$, where λ_{max} is the free space wavelength at the lowest frequency of operation). A prototype of the antenna is fabricated and tested. The simulated and measured S_{11} are in a good agreement. Measured radiation patterns confirm the pattern stability in terms of the direction of maximum radiation and 3 dB beamwidth.**

***Index Terms*—Ultrawideband (UWB) antennas, omnidirectional antennas, pattern stability, cable effect.**

I. Introduction

A broad spectrum of antennas for ultrawideband (UWB) systems has been studied in the past. The antennas for UWB channel sounding should have both large impedance bandwidth and stable radiation pattern. Actually, this is a major issue for UWB channel sounding, namely, the provision of an antenna with a stable radiation pattern over the entire impedance bandwidth. The current distribution on the antenna determines the shape of the radiation pattern. However, this distribution is frequency dependent and hence the maintenance of a constant radiation pattern over a broad frequency band (e.g. several GHz and more) is a serious challenge. Hereof, in the case of UWB channel sounding antennas the pattern stability means that the direction of maximum radiation is fixed or slightly varies with frequency. Furthermore, both maximum value of the gain and 3 dB beamwidth have to change in a narrow range while the side lobes in the radiation pattern have to be low compared to the main lobe over the covered spectrum. The realization of an antenna which meets these requirements allows a channel illumination in a similar way over a broad frequency band.

Classical examples of UWB omnidirectional antennas are biconical and discone antenna [1]. A biconical antenna operating over the frequency band 3.1-10.6 GHz has been presented in [2]. The antenna bandwidth is increased by adding a capacitive load to the cones and an inductive load between the cones by means of shorting pins. However, this enhancement of the bandwidth leads to both deteriorated symmetry and highly frequency dependence of the radiation pattern. In [3], a stacked biconical antenna covering the frequency range 26.2-30.2 GHz has been proposed. The radiation pattern of this antenna exhibits high ripples in both azimuth and elevation plane and also poor omnidirectivity. A design of stacked biconical antenna for the frequency band 3-20 GHz has been shown in [4]. In [5], a double discone antenna can be found operating in the frequency range 0.18-18 GHz. A skeletal discone antenna covering the spectrum 0.4-16.4 GHz has been proposed in [6]. However, the designs in [5] and [6] have tilted radiation patterns due to the asymmetric structure of the discone antenna and also show great frequency dependence.

In this letter, we present a compact antenna for UWB channel sounding. Each arm of the proposed antenna composes three components: cone, ring and cylinder. The radiator is fed with a standard coaxial cable in which the TEM mode is only excited. The antenna covers the frequency range 1.5-41 GHz with S_{11} below -10 dB and has a stable omnidirectional radiation pattern. A prototype of the antenna is fabricated and measured in order to validate the simulation. Both simulated and measured results are in a good agreement. Therefore, the proposed antenna is capable to illuminate a channel in a similar way over a wide frequency band. All studies were carried out with CST Microwave Studio [7].

II. Antenna Design Considerations

The cross section of the antenna is shown in Fig. 1(a). The design is based on a symmetrical biconical antenna. The latter is a modification of the dipole antenna in which the cylindrical conductors are replaced with conical ones. Theoretically, if the cones are infinitely long, then the impedance bandwidth is unlimited. However, the bandwidth of a biconical antenna with a finite length is limited and the lower bound of the covered band is normally controlled by the length of each cone while the upper one by the feed region size [1], [2].

The proposed antenna structure has a total size of 58 mm x 58 mm x 54 mm (the electrical dimensions are $0.29\lambda_{max}$ x $0.29\lambda_{max}$ x $0.27\lambda_{max}$ at the lowest frequency of operation) and is composed of two identical arms. The modification of the biconical antenna is carried out by adding a ring and a cylinder to each cone as seen in Fig. 1(a). The function of these elements is to reduce the influence of the cable effect on the antenna radiation pattern. The cable effect distorts the antenna radiation pattern through two mechanisms. First, the attached cable is in the antenna near field region and scatters or reflects part of the radiated field. Second, the current flowing on the outer surface of the cable shield causes radiation from the cable which in turn corrupts the antenna radiation pattern. This impact is considerable at lower frequencies. Thus, the cable effect changes the radiation pattern and ignoring the cable in the simulation (directly feeding the antenna with a signal source) can result in serious discrepancies between the simulated and measured results [8], [9].

The authors are with the Department of Electronic Systems, Faculty of Engineering and Science, Aalborg University, Aalborg, Denmark (e-mail: stz@es.aau.dk; ata@es.aau.dk; gfp@es.aau.dk).

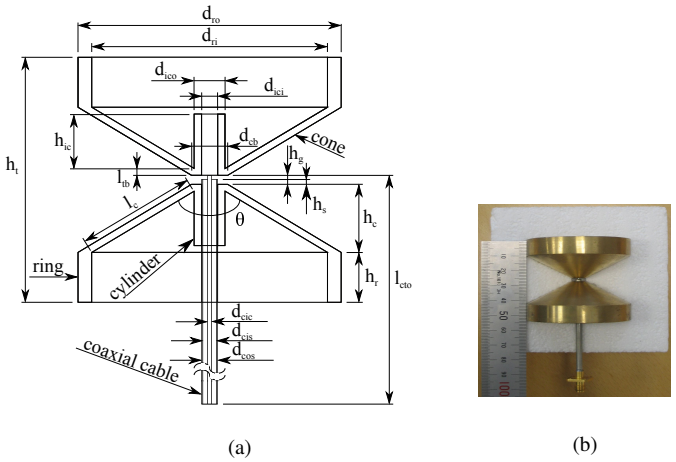

(a) (b)

Fig. 1. Proposed antenna: (a) cross section of the antenna fed with a coaxial cable and (b) antenna prototype placed in the polystyrene holder.

To study the influence of the cable on the antenna radiation pattern and to optimize the structure, before manufacturing, a standard 50-Ω coaxial cable is used for feeding the antenna as shown in Fig. 1(a). The cable inner conductor excites the upper arm and the cable shield is connected to the lower arm. The dielectric insulator between the conductors is teflon with a relative permittivity of 2.1 and a loss tangent of 0.0002. In the simulation the cable length was set to l_{cto} = 130 mm which is sufficient for determining the distortion of the antenna performance due to the cable effect. All antenna dimensions are shown in Table I.

TABLE I. Design dimensions of the proposed antenna

Symbol	Value	Symbol	Value	Symbol	Value
h_t	54 mm	d_{ro}	58 mm	l_{tb}	1.5 mm
h_c	15 mm	h_{ic}	12 mm	l_{cto}	130 mm
h_r	11 mm	d_{ici}	3.58 mm	d_{cic}	0.91 mm
l_c	30 mm	d_{ico}	6.8 mm	d_{cis}	2.98 mm
d_{cb}	8 mm	h_g	2 mm	d_{cos}	3.58 mm
d_{ri}	52 mm	h_s	1.1 mm	θ	120°

III. Results and Discussion

The antenna was fabricated and a photo of the prototype is shown in Fig. 1(b). The prototype was milled out of brass with a Computer Numerical Control (CNC) machine. This material was selected since it is easy to soldering and thus can be provided a good electrical connection between the antenna and cable. The CNC machine was also employed to make a holder of polystyrene and so to give a mechanical stability of the antenna. Thus, it is relieved the stress of the cable inner conductor which was keeping the weight of the top arm.

Fig. 2 shows the simulated and measured S_{11}. As one can see, the results are in a good agreement and the covered frequency band is from 1.5 GHz to 41 GHz with S_{11} below -10 dB. However, the measured S_{11} shows that the upper limit is 43 GHz. The reasons for this enlargement of the impedance bandwidth are measurement errors and that at high frequencies the real cable has higher losses than the simulated one, which lead to lower values of the mismatch loss.

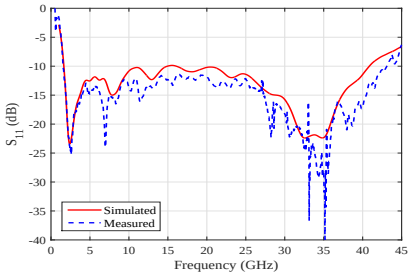

Fig. 2. Simulated and measured S_{11} of the proposed antenna.

To determine the effect of the antenna building elements on its impedance bandwidth, parametric studies are conducted. In each study all dimensions, except the varied one, are the same as presented in Table I. Fig. 3(a) shows the effect of the cylinders and rings on S_{11}. The cylinders effectively make the cones appear to have a greater angle θ and thus the input impedance shifts closer to 50 Ω. This results in an improved matching but the lowest operation frequency is increased with around 200 MHz compared to that of the antenna without cylinders and rings (standard biconical antenna). The introduction only of rings shifts the lowest useful frequency from 2.1 to 1.8 GHz since the rings increase the length of the arms which in turn determines that frequency. The simultaneous addition of both rings and cylinders lower the lowest operating frequency with about 600 MHz compared to the case without them. In order to verify the above analysis, a comparison of the input impedance in all cases is shown in Fig. 4. As one can see, the introduction of the cylinders and rings improves both real and imaginary part of the impedance at low frequencies (except in a narrow band around 2.5 GHz). By varying the cone length l_c from 20 mm to 40 mm the lower limit of the covered band decreases from 2.2 GHz to 1.3 GHz (not shown). However, the extension of the cones for an enlargement of the impedance bandwidth should be done carefully since it leads to a splitting of the main lobe in the radiation pattern at lower frequencies and also increases the size of the structure. Fig. 3(b) shows the simulated S_{11} for different cone angles θ. The results demonstrate that by sweeping the cone angle from 100° to 140° the lower limit of the covered band shifts from 1.35 GHz to 2.3 GHz. Therefore, the lowest operating frequency decreases with decreasing cone angle, but the matching in the band 15-20 GHz deteriorates and S_{11} crosses the limit of -10 dB. The data shows that the optimum performance is obtained for θ = 120°. To evaluate the impact of the gap distance h_g between the cones, its value is varied from 1.5 mm to 2.5 mm. From the results shown in Fig. 3(c) one can see that the lowest operating frequency for different gap distances is similar. However, the variation of the gap distance causes large changes in the matching and the optimum results are obtained for h_g = 2 mm. Another parameter influencing the impedance bandwidth is the height of the coaxial cable shield h_s above the lower arm to which it is attached. As can be seen in Fig. 3(d), small changes in h_s cause significant differences in the matching. The largest covered spectrum is obtained in the case of h_s = 1.1 mm.

Due to the rotational symmetry of the proposed antenna,

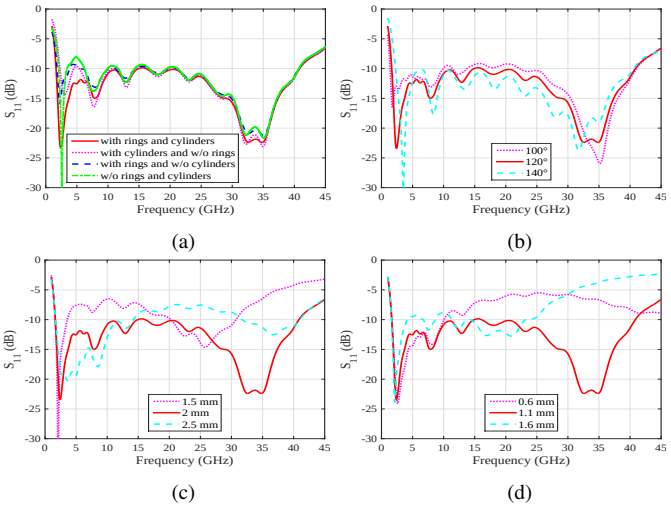

Fig. 3. Simulated S_{11} for: (a) antenna with rings and cylinders (proposed antenna), antenna with cylinders and without rings, antenna with rings and without cylinders, and antenna without rings and cylinders, (b) different cone angle θ, (c) different gap distance h_g, and (d) different height of the cable shiled above the cone h_s.

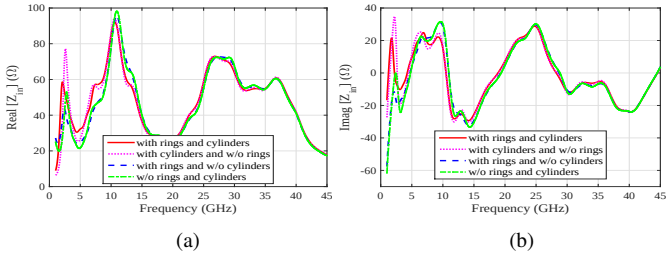

Fig. 4. Simulated (a) real and (b) imaginary part of the input impedance of: antenna with rings and cylinders (proposed antenna), antenna with cylinders and without rings, antenna with rings and without cylinders, and antenna without rings and cylinders.

its radiation pattern is omnidirectional in the azimuth plane (H-plane) and for the pattern stability can be judged from the elevation plane (E-plane). Fig. 5 shows simulated and measured normalized E-plane radiation patterns. Since the Aalborg university anechoic chamber can operate up to 22 GHz, this is the last frequency on which there is a measurement. The measured and simulated results in Fig. 5 are in a good agreement. As one can see at 2 GHz the shape of the radiation pattern is similar to this of a 0.5λ dipole, while at 6 GHz similar to the radiation pattern of a 1.25λ dipole. However, at 2 GHz the direction of maximum radiation is slightly shifted from 90°. The reason is that the cable effect is very strong at low frequencies due to the large current flowing on the cable shield. In other words, although the influence of the cable effect on the antenna performance is significantly reduced, it still has a small impact on the radiation pattern. With increasing frequency this influence diminishes, the direction of maximum radiation is not tilted and side lobes appear in the radiation pattern. However, the magnitude of the sidelobes is more than 5 dB lower than this of the main lobe. The simulated and measured results reveal that the 3 dB beamwidth varies from 30° to 65° over the covered band. Due to the good agreement between the full-wave simulations and measurements below 22 GHz it can be expected that above

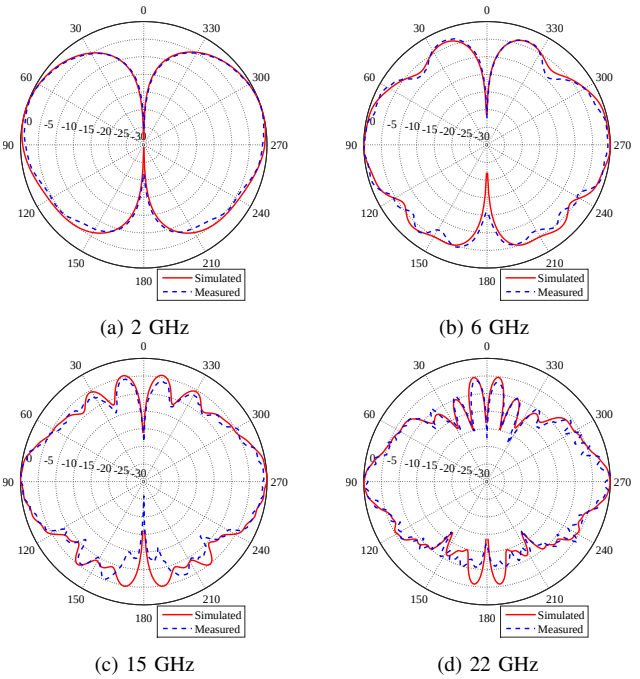

Fig. 5. Simulated and measured normalized E-plane radiation patterns of the proposed antenna.

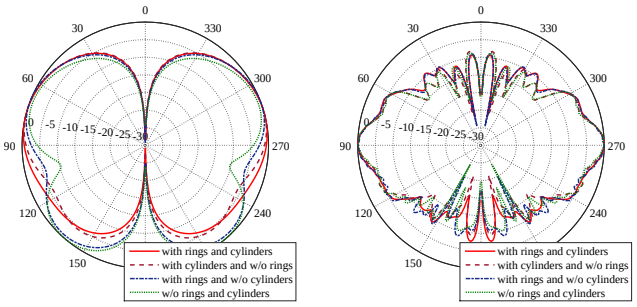

Fig. 6. Simulated normalized E-plane radiation patterns for the cases: antenna with rings and cylinders (proposed antenna), antenna with cylinders and without rings, antenna with rings and without cylinders, and antenna without rings and cylinders.

this frequency the antenna prototype will also have a stable omnidirectional radiation pattern similar to the simulated one (the simulated pattern at the highest operating frequency of 41 GHz can be seen in Fig. 8(b)).

Fig. 6 shows the simulated normalized E-plane radiation patterns of the proposed antenna (antenna with rings and with cylinders) and its variations: antenna with cylinders and without rings, antenna with rings and without cylinders, and antenna without rings and cylinders (standard biconical antenna). As one can see, without rings and cylinders the radiation pattern is strongly distorted at low frequencies due to the cable effect. The cases with only rings and with only cylinders show a better performance. The optimum results are obtained when rings and cylinders are simultaneously introduced. The suppression of the cable influence on the radiation pattern is a consequence of the reduction of the current flowing on the cable shield obtained by adding the rings and cylinders as shown in Fig. 7. As one can expect the surface current magnitude on the cable shield is highest in the

case of antenna without rings and cylinders. The introduction of either rings or cylinders leads to reduction and the lowest surface current magnitude on the cable shield is obtained when both types of elements are simultaneously employed. More precisely, both ring and cylinder which are part of the antenna lower arm alter the current distribution on it and therefore change the current on the cable shield, which is connected to that arm. By optimizing the dimensions of these elements the current distribution is changed so that the magnitude of the current flowing on the cable shield is decreased with more than 10 dB compared to the case without the extra elements. Thereby, the cable radiation is reduced and also the distortion of the radiation pattern. With increasing frequency the magnitude of the current flowing on the cable shield decreases and the cable impact becomes insignificant. Therefore, at high frequencies the radiation patterns for the different cases are similar as seen in Fig. 6. The simulated normalized E-plane radiation patterns of the proposed antenna for three scenarios: with straight cable, with bent cable at 90°, and without cable (directly fed with a signal source) are shown in Fig. 8. As one can see the presence of the cable has a little impact on the radiation pattern. In addition, the bending of the cable causes negligible changes in the radiation pattern.

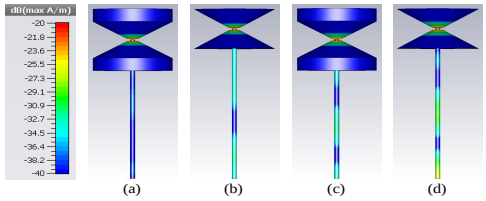

Fig. 7. Surface current distribution at 2 GHz for: (a) antenna with rings and cylinders (proposed antenna), (b) antenna with cylinders and without rings, (c) antenna with rings and without cylinders, and (d) antenna without rings and cylinders.

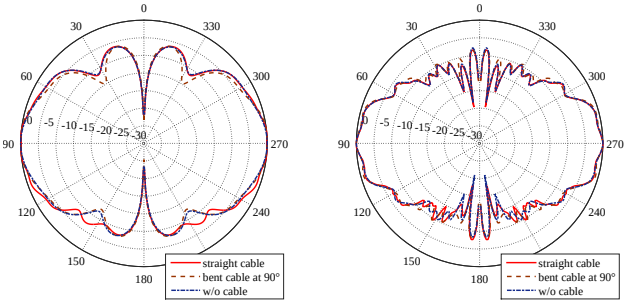

(a) 9 GHz (b) 41 GHz

Fig. 8. Simulated normalized E-plane radiation patterns of the proposed antenna for the cases: with straight cable, with bent cable at 90° and without cable (directly fed with a signal source).

Fig. 9 shows the simulated total efficiency (includes both radiation efficiency and mismatch loss) and realized gain of the antenna. Over the covered spectrum 1.5-41 GHz the antenna has high efficiency, and low gain changing slightly with frequency. An important requirement for UWB antennas is the group delay (indicates a quantity of a pulse distortion and far-field phase linearity) to be constant versus frequency or to show small deviations (the maximum variation should be less than 1 ns over the covered spectrum) [10]. By simulating two identical antennas placed at a distance of 1.8 m, it was found that the variation of the group delay is less than 0.8 ns over the whole covered frequency range.

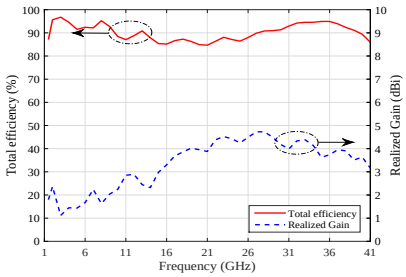

Fig. 9. Simulated total efficiency and realized gain of the antenna.

IV. Conclusion

A compact antenna for UWB channel sounding was presented in this letter. The antenna takes advantage of the wideband performance of a symmetrical biconical section. In order to reduce the influence of the cable effect on the antenna radiation pattern, a ring and a cylinder are added to each cone of the biconical section. By coupling the antenna with a coaxial cable and studying the cable impact in the simulation, the radiator is optimized to be robust against the cable effect. The simulated performance is verified by measuring the manufactured antenna prototype. The structure exhibits S_{11} below -10 dB and a stable omnidirectional radiation pattern over the frequency range 1.5-41 GHz. The obtained high total efficiency and stable gain also indicate a good antenna performance. These features allow similar illumination of a channel over a wide frequency range, which makes the proposed antenna very suitable for UWB channel sounding measurement campaigns.

References

[1] C. A. Balanis, *Modern Antenna Handbook*. Hoboken, NJ, USA: Wiley, 2008.

[2] A. K. Amert and K. W. Whites, "Miniaturization of the biconical antenna for ultrawideband applications," *IEEE Trans. Antennas Propag.*, vol. 57, no. 12, pp. 3728–3735, Dec. 2009.

[3] S. Liao, P. Chen, and Q. Xue, "Ka-band omnidirectional high gain stacked dual bicone antenna," *IEEE Trans. Antennas Propag.*, vol. 64, no. 1, pp. 294–299, Jan. 2016.

[4] N. Rostomyan, A. T. Ott, M. D. Blech, R. Brem, C. J. Eisner, and T. F. Eibert, "A balanced impulse radiating omnidirectional ultrawideband stacked biconical antenna," *IEEE Trans. Antennas Propag.*, vol. 63, no. 1, pp. 59–68, Jan 2015.

[5] K.-H. Kim, J.-U. Kim, and S.-O. Park, "An ultrawide-band double discone antenna with the tapered cylindrical wires," *IEEE Trans. Antennas Propag.*, vol. 53, no. 10, pp. 3403–3406, Oct. 2005.

[6] Y. Zhao and W. Wang, "Design of a novel broadband skeletal discone antenna with a compact configuration," *IEEE Antennas Wireless Propag. Lett.*, vol. 13, pp. 1725–1728, 2014.

[7] CST Microwave Studio, 2015 [Online]. Available: http://www.cst.com/.

[8] J. DeMarinis, "The antenna cable as a source of error in EMI measurements," in *Proc. IEEE 1988 Int. Symp. EMC, Symp. Record*, Aug. 1988, pp. 9–14.

[9] L. Liu, Y. F. Weng, S. W. Cheung, T. I. Yuk, and L. J. Foged, "Modeling of cable for measurements of small monopole antennas," in *Proc. Loughborough Antennas Propag. Conf. (LAPC)*, Nov. 2011, pp. 1–4.

[10] Y. J. Cho, K. H. Kim, D. H. Choi, S. S. Lee, and S.-O. Park, "A miniature uwb planar monopole antenna with 5-GHz band-rejection filter and the time-domain characteristics," *IEEE Trans. Antennas Propag.*, vol. 54, no. 5, pp. 1453–1460, May 2006.